Proceedings Paper:
Kienitz, K.H. and Kadirkamanathan, V. orcid.org/0000-0002-4243-2501 (2017) New insights for applications of Kreisselmeier's structure in robust and fault tolerant control. In: 2017 IEEE Aerospace Conference Proceedings. 2017 IEEE Aerospace Conference, 04-11 Mar 2017, Big Sky, MT, USA. IEEE . ISBN 9781509016136

https://doi.org/10.1109/AERO.2017.7943797

New Insights for Applications of Kreisselmeier's Structure in Robust and Fault Tolerant Control

Karl Heinz Kienitz
Instituto Tecnológico de Aeronáutica
12.228-900 São José dos Campos SP
Brazil
+55-12-3947-6931
kienitz@ieee.org

Visakan Kadirkamanathan
University of Sheffield
Sheffield S1 3JD
United Kingdom
+44-114-222-5680
visakan@sheffield.ac.uk

Abstract — **This paper addresses a two degree of freedom structure discussed by Kreisselmeier for the SISO case in 1999. The discussion herein considers a MIMO setting, and aims at the use of this control topology for robust and fault tolerant control. It is also shown how design barriers can be obtained for robust I/O transfer behavior assignment and robustness evaluation schemes can be devised which allow for the quantitative valuation of I/O transfer behavior degradation in the presence of plant model uncertainty. The concepts and techniques are illustrated and assessed using an in-flight simulation problem.**

TABLE OF CONTENTS

1. INTRODUCTION

In 1999, Kreisselmeier proposed the use of a special two degree of freedom control structure in linear control [1], demonstrating its advantages for SISO systems in the sense that: (a) it allows for a two step design in which the designer imposes I/O transfer behavior in a first design step, and then obtains disturbance as well as noise rejection in a second, independent step; (b) restrictions on admissible, achievable I/O (target) transfer behavior are given; and (c) the impossibility is demonstrated to overcome such restrictions with any other linear control strategy.

Kreiselmeier's work went largely unnoticed, presumably because it was not published in English. It was formulated in a SISO setting, geared towards the practicing engineer.

However, most of Kreisselmeier's insights carry over into a MIMO setting, as shown herein. Furthermore, association of the second design step with robust control design methods such as H∞ and TFL/LTR (generalization of the LQG/LTR approach) may result in excellent disturbance and noise rejecting loops, as well as possible tolerance of sensor or actuator loss under certain conditions [5].

The analysis presented in this paper aims at creating instruments for robust I/O transfer behavior assignment and for robustness evaluation schemes that can be devised for the quantitative valuation of I/O transfer behavior degradation in the presence of plant modelling error. The concepts and techniques are illustrated and assessed using an in-flight simulation problem.

This paper is organized as follows. In section 2 Kreissemeier's structure is revisited and analyzed. Controller design considering this structure is the topic of section 3. An application example statement (intended for illustration purposes) and application-oriented insights are given in section 4. Results for the example are found in section 5. Section 6 contains comments and conclusions.

2. TWO DEGREE OF FREEDOM STRUCTURE

The two degree of freedom structure proposed by Kreisselmeier [1] is defined in Figure 1. In his paper, Kreisselmeier discussed the SISO case. Most of his results and conclusions apply to the MIMO case, sometimes in some generalized form, as shown in what follows.

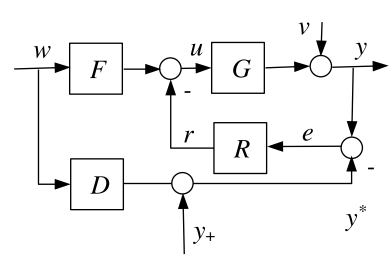

Figure 1. Two degree of freedom structure

In the structure proposed in Figure 1, w is a reference signal vector, v is a disturbance signal vector, y is the plant output vector, and y^* is a desired output vector resulting from the addition of a nominal desired transfer output Dw and an output addition vector y_+. D is the square transfer matrix of a reference model of the desired closed-loop dynamics. G is the transfer matrix of the linear plant with m inputs and p outputs, $m \geq p$, and such that G has linear independent rows. F is a feedforward compensator to be designed such that the input-output transfer matrix of the overall system is equal to D. R is a closed loop controller to be designed for loop stability, disturbance rejection, rejection, and robustness.

Theorem 1 – If $F=G^+D$, with $G^+=G^T(GG^T)^{-1}$, is chosen (i.e. $F=G^{-1}D$ in the case of $m=p$), the input-output transfer matrix of the structure defined in Figure 1 is D, independently of the choice of R.

Proof – For the output signal y the following equations hold:

$$y = Gu + v$$
$$y = G(Fw - Re) + v$$
$$y = G(Fw - Ry + RDw - Ry_+) + v$$

Thus

$$y = (I+GR)^{-1}(GF + GRD)w + (I+GR)^{-1}(GRy_+ + v) .$$

Since $F=G^+D$, one obtains

$$y = (I+GR)^{-1}(GG^+D + GRD)w + (I+GR)^{-1}(GRy_+ + v),$$

i.e.

$$y = Dw + (I+GR)^{-1}GRy_+ + (I+GR)^{-1}v. \qquad (1)$$

Because stability of F is a necessary condition for the internal stability of the system in Figure 1, for any practical purpose it is important to know what are the limitations on obtainable D. The following result from [2] provides a test for obtainable D when $m=p$, i.e. a test to verify if D is such that $F=G^{-1}D$ is stable. The result from [2] was adapted and recast using the notation adopted herein, as follows.

Theorem 2 – $F = G^{-1}D$ will be stable if and only if

$$\lambda_i^T D(z_i) = 0$$

for all RHP zeros z_i of the plant $G(s)$, where λ_i is such that

$$\lambda_i^T G(z_i) = 0 .$$

Remark: λ_i is a left eigenvector of $G(z_i)$ associated with the eigenvalue zero. λ_i has been termed a *zero direction* (of z_i) because a zero system output will result from any input with frequency z_i in the direction λ_i.

For the SISO case, the condition on Theorem 2 simplifies to the condition presented in [1], demanding that all RHP zeros of G must also be zeros of D.

In the view of Theorems 1 and 2, control design for the Kreisselmeier structure is a twostep process:

(a) choice of a desired transfer matrix D for the closed loop, satisfying the condition in Theorem 2; the stable F is then readily determined;
(b) the design of loop controller R to secure desired loop properties, such as disturbance rejection and robustness.

3. Loop Controller Design

The design of R can be accomplished through any suitable method that is capable of dealing with the set of given specifications entailed by an application of interest. Thus one can envision the use of the family of TFL/LTR methods [5] or H∞ norm based methods [3] involving requirements in terms of loop sensitivity $S=(I+GR)^{-1}$ and the complementary sensitivity $T=(I+GR)^{-1}GR$. Because of (1), these design methods will adequately address stability and disturbance (and also measurement noise) rejection requirements. However, it has so far been an open question how the transfer matrix of the structure in Figure 1 (which in the nominal case is D) is affected by plant uncertainty. To evaluate this issue, restrict plant G to be square and adequately described by a nominal plant model G_n affected by multiplicative output error (or uncertainty) E, as schematically represented in Figure 2. Assume further that G and G_n have normal full rank.

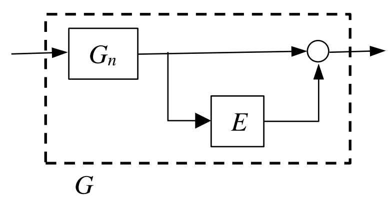

Figure 2. Plant affected by output multiplicative uncertainty

A common assumption on E (e.g. [3]-[6]) is that $E(s) = w_{unc}(s)\Delta(s)$, where w_{unc} is a scalar (transfer function) weight and Δ is an unknown but bounded transfer function matrix such that

$$\|\Delta\|_\infty \leq 1 .$$

Furthermore, often structure information on Δ may be available and is useful to better inform controller design [3].

Now one may write the following relations:

$$G = (I+E)G_n$$
$$G_n = (I+E)^{-1}G, G_n^{-1} = G^{-1}(I+E).$$

Hence

$$y = (I+GR)^{-1}(GG_n^{-1}D + GRD)w$$
$$y = (I+GR)^{-1}[(I+GR)+E]Dw$$
$$y = [I+(I+GR)^{-1}E]Dw$$

or

$$y = [I + E_S]Dw, \tag{2}$$

where

$$E_S = SE. \tag{3}$$

This means that, when using the Kreisselmeier structure with uncertain plants, one obtains the desired input-output transfer *D* with an output multiplicative error equal to the output multiplicative error *E* of the plant, filtered by the plant's sensitivity *S*. Thus, in the light of (1)-(3), the design of *R* should aim at the shaping of plant sensitivity considering information on disturbance vector *v*, output addition vector y_+, and modelling error (or uncertainty) *E*.

In the light of (1)-(3), performance and its robustness may be defined via demands on *T* and *S*. Such demands may be translated into approximate open loop requirements for *GR* (e.g. as in [4]). Thus, in frequency regions where small singular values of sensitivity $S(j\omega)$ are required, i.e. where

$$\sigma_{\max}[S(j\omega)] < \alpha_r(\omega) << 1, \omega \in \Omega_r,$$

this translates into the approximate open loop requirement

$$\sigma_{\min}[G(j\omega)R(j\omega)] > \frac{1}{\alpha_r(\omega)[1 - |w_{unc}(j\omega)|]}, \omega \in \Omega_r.$$

In frequency regions where small singular values of complementary sensitivity $T(j\omega)$ are required, i.e.

$$\sigma_{\max}[T(j\omega)] < \alpha_n(\omega) << 1, \omega \in \Omega_n,$$

this translates into the approximate open loop requirement

$$\sigma_{\max}[G(j\omega)R(j\omega)] < \frac{\alpha_n(\omega)}{[1 + |w_{unc}(j\omega)|]}, \omega \in \Omega_n.$$

To illustrate the design along the guidelines outlined above, a linear in-flight simulation example is now considered.

4. Application Example And Insights

In the illustrative application example considered here, the plant *G* and the desired transfer behavior *D* are, respectively, linearized models of the Dornier 328 aircraft (Do 328) [7] and that of a benchmark aircraft model labelled RJX, intended for prospective studies, with the typical dynamical behavior of a 120 passenger regional aircraft [8].

The state variables of both linear models are those describing the latero-directional motion of an aircraft (not necessarily in the order below):

$\Delta\beta$: variation of sideslip angle
$\Delta\phi$: variation of roll angle
Δp: variation of roll rate
Δr: variation of gear rate

The input to the system are the deflections of the ailerons, $\Delta\delta_a$, and the rudder, $\Delta\delta_r$. The outputs, measurements and controlled variables are Δp and Δr.

G and *D* resulted from the linearization on cruise operation points. As both aircraft are of different size, models are taken on different Mach and different altitudes. An advantage of in-flight simulation is precisely that simulation is carried out under physically different conditions from those assumed for the simulated dynamics.

The purpose of the in-flight simulation is to yield a response of the controlled outputs of the smaller plane close to the expected outputs of the larger plane and therefore show the ability to simulate the desired dynamics. Although in-flight simulation has been used for many years [9]-[11], it continues to be an active field of applied research [12],[13].

4.1. Block D – RJX Aircraft Model

This is a linear RJX model, stemming from linearization at flight conditions 0.8 Mach and 6096 m altitude. The linear model is the same used in [8]. The nonlinear model will not be discussed herein. The matrices for the linear state and output equations of this block are:

$$A_D = \begin{bmatrix} -0.2695 & -4.4527 & -250.96 & 9.8054 \\ -0.1089 & -3.1944 & 1.3789 & 0 \\ 0.0286 & 0.0274 & -0.5583 & 0 \\ 0 & 1 & -0.0149 & 0 \end{bmatrix}$$

$$B_D = \begin{bmatrix} 0 & 18.167 \\ -5.8631 & 0.6586 \\ -0.1734 & 3.1313 \\ 0 & 0 \end{bmatrix}, C_D = \begin{bmatrix} 0 & 1 & 0 & 0 \\ 0 & 0 & 1 & 0 \end{bmatrix}, D_D = 0_{2\times2}$$

4.2. Block G – Do 328 Aircraft Model

This is a linear DO 328 model, linearized at Mach 0.428 and altitude 900 m. This model was obtained from (Brockhaus *et al.*, 2011). The matrices for the linear state and output equations of block *G* are:

$$A = \begin{bmatrix} -0.87 & -6.47 & -0.411 & 0 \\ -1 & -0.376 & 0 & 0.0681 \\ 0.913 & -18.8 & -3.91 & 0 \\ 0 & 0 & 1 & 0 \end{bmatrix}$$

$$B = \begin{bmatrix} 0.877 & -7.78 \\ 0 & 0.12 \\ -14.3 & 3.74 \\ 0 & 0 \end{bmatrix}, C = \begin{bmatrix} 0 & 1 & 0 & 0 \\ 1 & 0 & 0 & 0 \end{bmatrix}, D = 0_{2\times2}$$

4.3 Block F

This block was determined using $F = G^{-1}D$. In this application T and G both have zeros at the origin. In such situation the technique (i.e. this definition of F) was used after an incremental perturbation of the zeros into the left half plane.

4.4. Block R – Controller

To calculate the loop controller R, the TFL / LTR approach ([5],[6]) was used. A brief review of the approach follows.

The TFL / LTR (Target Feedback Loop / Loop Transfer Recovery) approach is used for the design of robust controllers of SISO and MIMO systems. The method operates in two stages, which consist of a quadratic filter gain calculation and an LQR (Linear Quadratic Regulator) gain calculation, as described in classical references, such as [4] and [5]. The most important features of the method are:

- The robustness of the controlled loop with respect to a broad class of modeling errors.
- The technique has been designed for application to multivariable systems.
- The methodology is based on a frequency approach to linear time-invariant systems.
- The number of design parameters is relatively small.

To be used in the context of Figure 1, R was designed as a TFL/LTR controller for the liner plant G, whose state representation is defined by the data given in subsection 4.2.

A block diagram of R designed via the TFL/LTR approach is given in Figure 3, where I stands for the identity matrix, and H and K are respectively a quadratic filter gain and a LQR gain to be calculated as indicated in what follows.

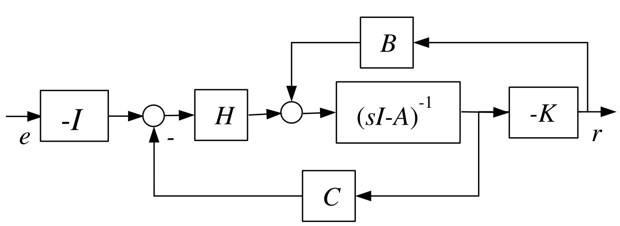

Figure 3. TFL/LTR controller to be used as loop controller *R* in the systems of Figure 1

Firstly, gain matrix H is determined so that a dynamic as in Figure 4 has loop properties relevant to the application. This dynamic is called the target feedback loop (TFL) dynamics for the GR loop in Figure 1.

In a second step (called Loop Transfer Recovery, LTR) the gain matrix K, is determined such that the loop dynamics (herein the dynamics of the GR loop in Figure 1) is as close as possible to the target feedback loop dynamics.

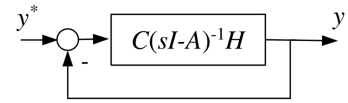

Figure 4. Target feedback loop dynamics for the *GR* loop in Figure 1

The equations used herein for calculating H are those used for calculating gains in LQG filtering problems. The equations for calculating G are those used in calculating the gain LQR problems. The choices are motivated by considerations of algebraic convenience and of robustness (see [4], [5] and references therein).

The design equations to be solved for the determination of H (and desired dynamics of Figure 4 and the GR loop in Figure 1) are:

$$H = \frac{1}{\mu}\Sigma C^T \tag{4}$$

$$A\Sigma + \Sigma A^T + LL^T - \frac{1}{\mu}\Sigma C^T C\Sigma = 0 \tag{5}$$

The design parameters are the matrix L and the scalar μ. Σ is a symmetric positive definite solution of the algebraic Riccati equation (5). Common choices for L are B or $AC^T(CC^T)^{-1}$ [4].

For the second step (calculation of gain K), the equations are:

$$G = \frac{1}{\rho}B^T P \tag{6}$$

$$A^T P + PA + C^T C - \frac{1}{\rho}PBB^T P = 0 \tag{7}$$

The ρ parameter defines the quality of recovery, which is the degree of proximity of GR and for this purposed must be made as small as necessary. P is a symmetric positive definite solution algebraic Riccati equation (7).

Finally, the transfer matrix of the controller R is:

$$R(s) = K(sI - A + BK + HC)^{-1}H \qquad (7)$$

[4] and [5] discuss other two step design calculation schemes that apply to controllers of the type shown in Figure 3. Such design calculation schemes feature modified or different design equations, which in the case of stable plants lead to loops that are robustly stable with respect to loss of sensors or loss of actuators, making them particularly suitable in fault tolerant control settings. The requirement for a stable plant can be met by a preliminary stabilization with some inner loop controller that uses actuators and sensors of highest

dependability. Thus, the adequate combination of control design schemes with the Kreisselmeier structure provides a control framework most suitable for robust and (robust control inspired) fault tolerant control. The interest of the Kreisselmeier structure for fault-tolerant control has already been pointed out elsewhere in a different setting [14].

4.5. Preliminaries on the Design Evaluation

For the evaluation of the design results through simulation, actuator saturation (±10º) and rate saturation (±40º/s) of the actuators were added to *G*, as well as measurement noise on both channels. The evaluation simulation emulates the use of a Do 328 aircraft flying in still air to simulate the dynamic response of the RJX dynamics, subject to a disturbance crosswind. This is a typical in-flight simulation scenario [10]. Figure 5 schematically describes the implemented simulation.

The simulation includes: (a) a 5° doublet input command (sequence of a positive pulse followed by a negative pulse); and (b) an artificial disturbance signal of step type at 25s simulation time, simulating a lateral wind step of 10 knots on the dynamics of RJX (but not on the dynamic simulator Do 328). Note that the adequate response to the simulated wind gust and to measurement noise must be enforced by the convenient, frequency selective shaping of the complementary sensitivity function, because both signals enter through the output addition vector y_+.

For consideration of the simulated wind gust $d(t)$, an augmented state equation representation for *D* is used, following the procedure adopted in [15]:

$$\dot{x}_D(t) = A_D x_D(t) + B_D u_D(t) + B_d d(t), B_d = \begin{bmatrix} -0.0009 \\ -0.1089 \\ 0.0286 \\ 0 \end{bmatrix}$$

$$y_D(t) = C_D x_D(t)$$

5. Results

Figure 6 shows the frequency response of the open loop dynamics desired for *GR*. The choice of design parameters was $\mu = 0.1$ and $L = AC^T(CC^T)^{-1}$, which is an option in equations (4)-(5) to obtain matched singular values in low frequency [4]. Figure 6 also shows a design barrier for robust stability with respect to modeling error (or uncertainty) of the type defined in Figure 2. $w_{unc}(s) = s/(s+50)$ was adopted, which accounts for generic output multiplicative uncertainty dominated by first order dynamics with time constant smaller than 0.13 s. From TFL / LTR design considerations (see e.g. [4]), the robust stability design barrier not to be violated is $1/|w_{unc}(j\omega)|$.

Applying the considerations summarized in section 3 to this application, small singular values of $S(j\omega)$ are required for model following immunity to modeling error, in the frequencies of interest, i.e. in frequencies within the bandwith of *D* (aprox. 7 [rd/s]). Furthermore, because $S+T=I$, small singular values of $S(j\omega)$ are also required for good tracking of the output addition vector in low frequencies, in order to correctly simulate the response to the artificial wind step.

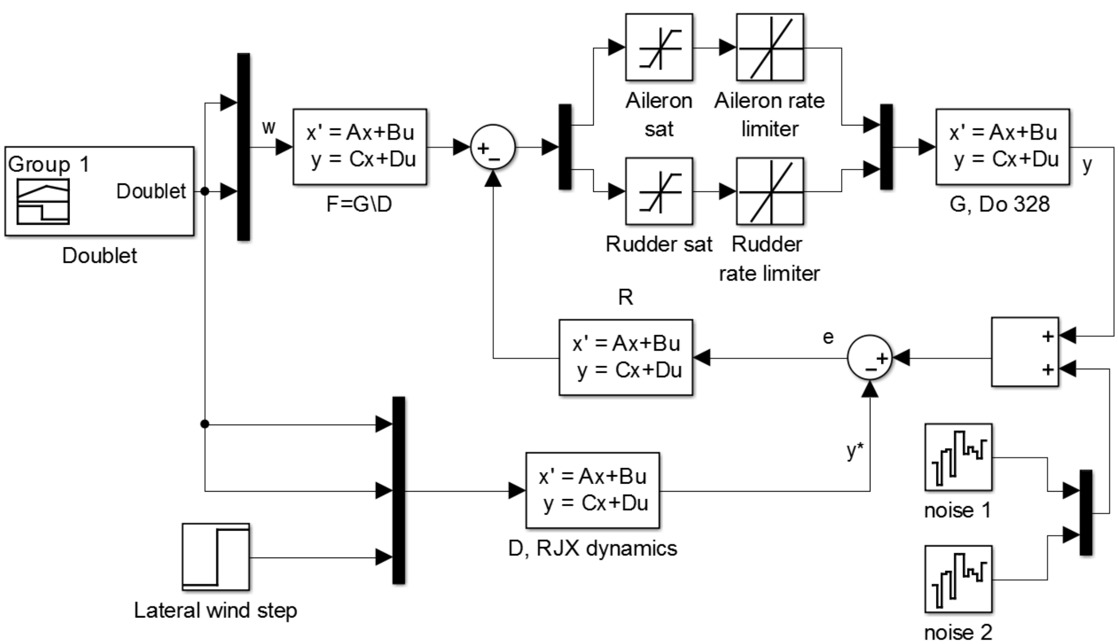

Figure 5. Implementation of the evaluation simulation in Matlab / Simulink.

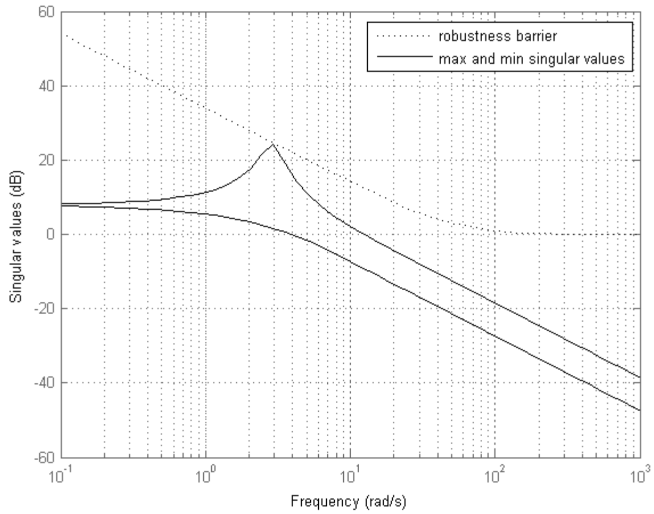

Figure 6. Target frequency response for *GR*, obtained with the choices μ = 0.1 and $L = AC^{\mathrm{T}}(CC^{\mathrm{T}})^{-1}$

Results of the loop transfer recovery step are shown in Figure 7. The singular values of $G(j\omega)R(j\omega)$ are close to those of $C(sI - A)^{-1}H$ for $\rho = 0.001$.

Figures 8 and 9 show the roll and gear responses to a 5º, doublet maneuver at 10 s and a step corresponding to a lateral 10 knots wind at 25s on the (simulated) RJX dynamics. In these figures, the solid line gives the plant's response, i.e. that of *G* (Do 328), simulation output. The dotted line gives the desired, i.e. ideal response of *D* (RJX), which is the response of the dynamics to be simulated in the in-flight simulation with the best approximation possible.

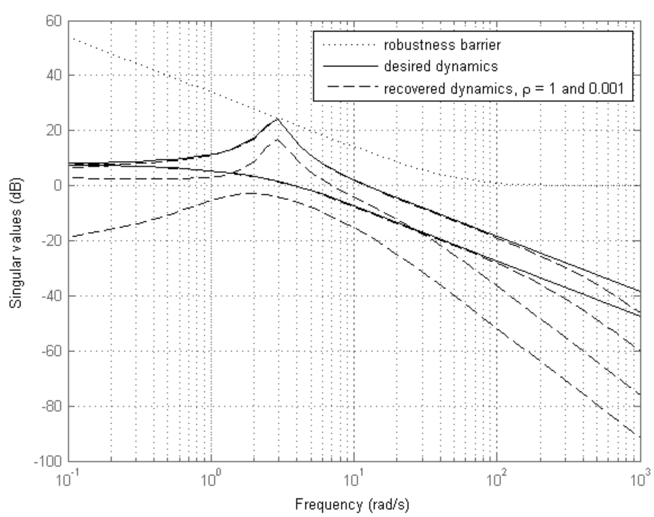

Figure 7: Frequency response of the target dynamics and the recovered (open) loop

Finally, the use of ailerons and rudder is given in Figure 10. Given the doublet input and the atmospheric disturbance, control surface use remained within operationally acceptable limits.

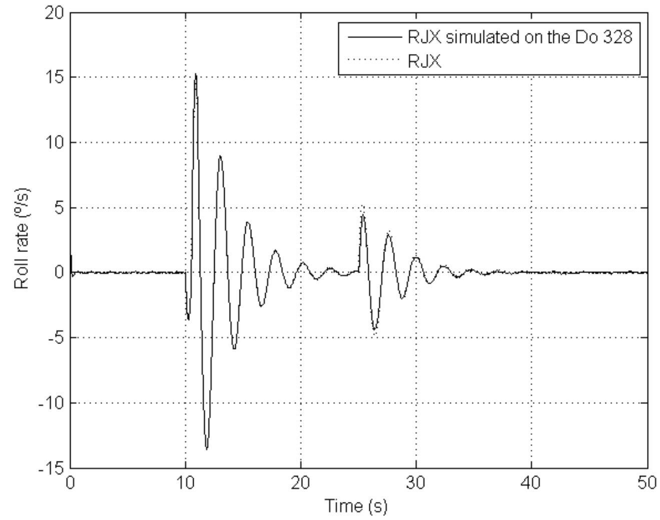

Figure 8: Responses of the simulation and of the dynamics to be simulated: roll rate

6. Comments and Conclusion

The Kreisselmeier structure was revisited with MIMO considerations on several of its features. As application illustration an in-flight simulation problem was addressed. Using the Kreisselmeier structure and a TFL/LTR controller, a chosen hypothetical aircraft behavior was enforced with good approximation on another aircraft. The results illustrated the qualities and feasibility of the proposal.

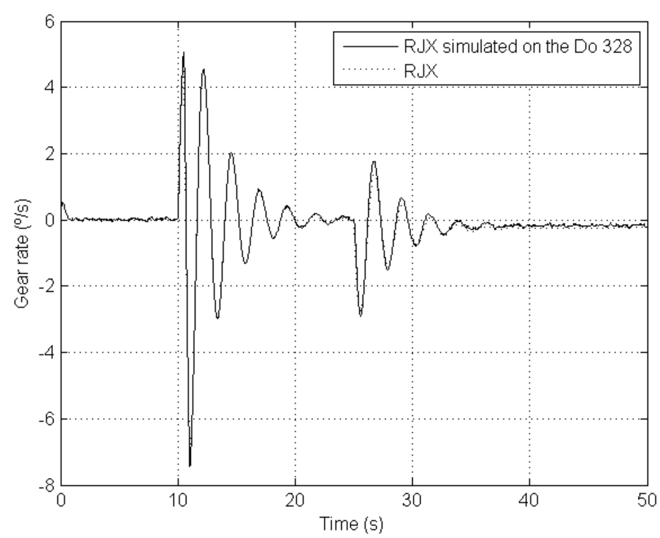

Figure 9: Responses of the simulation and of the dynamics to be simulated: gear rate

The loop design considerations given in section 3 addressed the basic issues in a framework which made use of a TFL/LTR approach. Herein this method was chosen for its simplicity and sufficiency in presenting a good illustration of the relevant features. More elaborate design methods such as

H∞ and structured singular value based methods [3] may allow for the use of structure information on $E(s)$, if available. Further work by the authors is addressing this issue.

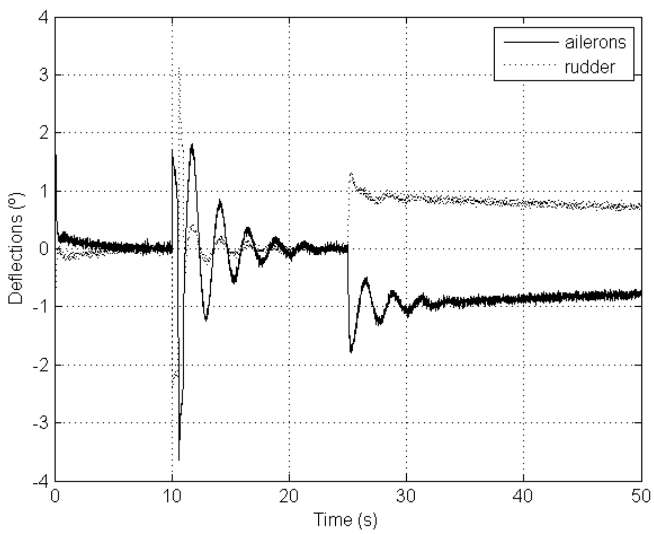

Figure 10: Aileron and rudder deflection history

Additional work may address in-flight simulation issues as may appear in different simulation scenarios. While in the illustrative example a simulated wind disturbance (injected during flight through calm air) was considered, in-flight simulation in disturbed air is also of interest. In situations in which the disturbance is not simulated but consists of a burst of true wind, two scenarios can be envisioned: a simpler one, in which the (actual) disturbance is not measured, and a more elaborate one in which a sensor measures the disturbance. Although not yet commonly considered, this second scenario is feasible in the current state of the art [16]. In all these in-flight simulation applications, the Kreisselmeier structure can be used with the advantages described in this paper.

ACKNOWLEDGEMENTS

The support of the followings institutions is gratefully acknowledged: FAPESP (grant 2011/17610-0) and CAPES (grant 88887.125251/2015-00).

REFERENCES

[1] Kreisselmeier, G., 1999. Two-degree-of-freedom control structure. *at-Automatisierungstechnik*, v. 47, 266-269.

[2] Morari, M, Zafiriou, E, Holt, B.R., 1987. Design of resilient processing plants. New characterization of the effect of RHP zeros. *Chemical Engineering Science*. v. 42, p. 2425-2428.

[3] Skogestad, S. and Postlethwaite, I., 1996. *Multivariable Feedback Control – Analysis and Design*, John Wiley.

[4] Cruz, J.J., 1996. *Controle robusto multivariável*. EDUSP, São Paulo.

[5] Prakash, R., 1990. Target Feedback Loop/Loop Transfer Recovery (TFL/LTR) robust control design procedures. *Proc. 29th IEEE Conference on Decision and Control*, p. 1203-1209.

[6] Prakash, R., 1992. Robust control of an induction motor drive with Lyapunov Filter and Linear Quadratic Regulator. *Proc. 31st IEEE Conference on Decision and Control*, p. 1725-1731.

[7] Brockhaus, R., Alles, W., Luckner, R., 2001. *Flugregelung*. 3rd Ed., Springer.

[8] Martins, L.S.; Moreira, F.J.O.; Kienitz, K.H., 2014. Contribuições à simulação em voo usando a topologia de controle de Kreisselmeier e controle LQG/LTR. *XXI Congreso de la Asociación Chilena de Control Automático - Actas del Congreso*. p. 291-298, Santiago, Chile.

[9] Shafer, M. F., 1993. In-flight simulation studies at the NASA Dryden Flight Research Facility. NASA Ames Research Center, *1993 Technical Paper Contest for Women*. Paper 94N35969, p 77-97.

[10] Bauschat, J.-M., 2002. Long-term flight-test experience: a nonlinear in-flight simulation approach. *Proc. AIAA Modeling and Simulation Technologies Conference and Exhibit*, Paper AIAA-2002-4600, Monterey, USA.

[11] Weingarten, N.C., 2005. History of in-flight simulation at General Dynamics. *Journal of Aircraft*, v. 42, p. 290-298.

[12] Sato, M., Satoh, A., 2008. Simultaneous realization of handling and gust responses: in-flight simulator controller design. *Journal of Guidance, Control and Dynamics*, v. 31, p. 1545-1560.

[13] Ko, J.S., Park, S., 2014. Variable stability system control law development for in-flight simulation of pitch/roll/yaw rate and normal load. *International Journal of Aeronautical & Space Science,* v. 15, p. 412–418.

[14] Ding, S.X., 2009. Integrated design of feedback controllers and fault detectors. *Annual Reviews in Control*, v. 33, p. 124-135.

[15] Nelson, R.C., 1998. *Flight stability and automatic control*, 2nd Ed., McGraw-Hill.

[16] Hahn, K.U, Schwartz, C., 2008. Alleviation of atmospheric flow disturbance effects on aircraft response. *Proc. 26th Congress of the International Council of the Aeronautical Sciences*. Paper ICAS 2008-5.2.2, Anchorage, Alaska.